Fluid Mixing for Low-Power 'Digital Microfluidics' Using Electroactive Molecular Monolayers

Maria Serena Maglione, Stefano Casalini, Stamatis Georgakopoulos, Marianna Barbalinardo, Vitaliy Parkula, Nuria Crivillers, Concepció Rovira, Pierpaolo Greco, Marta Mas-Torrent

M. S. Maglione, Dr. S. Casalini, Dr. S. Georgakopoulos, Dr. N. Crivillers, Prof. C. Rovira, Dr. M. Mas-Torrent
Institut de Ciència de Materials de Barcelona (ICMAB-CSIC) and CIBER-BBN, Campus UAB, 08193 Bellaterra (Spain).
E-mail: mmas@icmab.es

Dr. M. Barbalinardo
Istituto per lo Studio dei Materiali Nanostrutturati, CNR. Via P. Gobetti 101 Bologna.

Dr. M. Barbalinardo, V Parkula, Dr. P. Greco
Scriba Nanotecnologie srl, via di Corticell 183/8, 40128 Bologna (Italy).
E-mail: pgreco@scriba-nanotec.com

Keywords: self-assembled monolayer, electroactive molecule, quinone, electrowetting, microfluidics

A switchable electrode, which relies on an ITO conductive substrate coated with a self-assembled monolayer terminated with an anthraquinone group (AQ), is reported as an electrowetting system. AQ electrochemical features confer the capability of yielding a significant modulation of surface wettability as high as 25° when its redox state is switched. Hence, an array of planar electrodes for droplets actuation was fabricated and integrated in a microfluidic device to perform mixing and dispensing on sub-nanoliter scale. Vehiculation of cells across microfluidic compartments is made possible by taking full advantage of surface electrowetting in culture medium.

1. Introduction

Self-assembled monolayers (SAMs) of molecules bearing a functional terminal group covalently linked to technologically relevant surfaces such as Au or metal oxides have been widely used to tune the surface properties.[1] In particular, SAMs tailored with a redox active terminal group have arisen great interest because they can shed light into the mechanisms of the heterogeneous electron transfer as well as for the fabrication of electrochemical switchable systems.[2-6] For instance, SAMs based on ferrocene,[7-8] fullerene,[9] tetrathiafulvalene, [10] porphyrin,[11] and quinone[12-15] have been successfully exploited in a wide spectrum of applications including charge storage, cells guidance, protein grafting and charge transport. Further, several groups have unambiguously demonstrated that inert[16,17] and redox-active SAMs[18-21] can be efficiently used to modify the surface energy when a voltage is applied to them. Inert SAMs act as insulating dielectrics; hence the capacitive charging at its surface is the effective driving force for water actuation. On the other hand, electroactive SAMs yield the same result due to the faradaic switch of the terminal group, whose redox state changes and, consequently, its charge or polarizability.[22] Such surface wettability modification has been previously exploited for capturing/releasing biomolecules as well as for re-shaping water droplets.[23]

In the field of digital microfluidics, different physical phenomena can be exploited in order to replace the standard mechanical pumping of aqueous samples, such as electro-osmosis,[24-25] electrowetting,[26] electrohydrodynamic pumping[27-29] and electrothermal flow.[30,31] Within this context, electrowetting-on-dielectric (EWOD) [32] has been successfully implemented into microfluidics[33-37] because it permits the control over shape and flow of droplets by applying well-defined electrical fields.[38] EWOD is based on the application of a voltage between an electrode and a conductive droplet separated by a dielectric film. Such bias between the driving and counter electrode gives rise to the dielectric polarization, which promotes the droplet actuation. Typically, this is achieved through two different configurations: i) the “single-plate” and ii) “two-plate” device.[39] One of the hot-topics within this field is focused

on lowering the driving potential in order to develop low-power and disposable actuators.[40] As a result, since the fabrication of the first devices, the driving potentials have been dramatically reduced from ±100 V to 10 V.[41] Electroactive SAMs able to switch significantly the surface energy, and hence its wetting properties, at very low voltages can offer thus an alternative and unprecedented route for their application in low-voltage operation digital microfluidics.[42]

Here, we use an anthraquinone (AQ)-terminated SAM covalently grafted on a transparent indium-tin oxide (ITO) substrate in order to yield controlled gradients of wettability for the electrochemical actuation of aqueous droplets. To the best of our knowledge, this is the first time that an AQ-based SAM has been successfully implemented into a full-standing chip composed by an array of planar electrodes together with a microfluidic system. Its principal features are the following ones: i) full transparency, ii) high throughput, iii) low operational voltage (*i.e.* from ≈3 V down to hundreds of mV) and iv) bio-friendliness. This last feature was benchmarked against droplets containing mouse embryonic fibroblast cells NIH-3T3. Thus, this work shows unambiguously that AQ-based SAMs are highly appealing in the field of digital microfluidics.

2. Experimental

2.1 Chemicals

9,10-dioxo-N-(3-(triethoxysilyl)propyl)-9,10-dihydroanthracene-2-carboxamide (AQSi) was synthesized as reported in literature[43] in 70% yield following the procedure shown in Scheme 1. 10-undecenyltrichlorosilane (UTCS) was purchased from abcr GmbH and was used without further purification. Polyester acrylic double sided adhesive 9096 was purchased by 3M. Dulbecco's modified Eagle medium (DMEM), nutrient mixture F-12, trypsin-EDTA,

L-glutamine and penicillin-streptomycin were purchased from Sigma Aldrich. Fetal bovine serum (FBS) was purchased from Gibco^{TM}.

2.2 Protocols for substrate activation and SAM formation

ITO-coated glass slides (25 mm x 25 mm x 0.55 mm) were purchased from Delta Technologies. These substrates were systematically cleaned by sonicating them for 15 minutes in a series of solvents: dichloromethane, acetone and ethanol (HPLC pure grade). The substrates were then activated with an UV-ozone cleaner (exposure time equal to 20 min) and used immediately for their functionalization. For the preparation of electroactive AQSi-SAMs, the substrates were immersed in a 0.5 mM solution of AQSi in toluene for 12 hours, while for fabricating the control UTCS-SAMs they were inserted in a solution of UTCS 1% in toluene for 1 hour. The functionalized substrates were rigorously rinsed with toluene to avoid physisorption of the molecules and then dried with a nitrogen flow.

2.3 Electrochemical measurements

The measurements of cyclic voltammetry (CV) and linear sweep voltammetry (LSV) have been carried out using a potentiostat/galvanostat 263a (EG&G Princeton Applied Research). A conventional three-electrode setup was used in both cases. The modified ITO substrate was used as the working electrode (WE), while a platinum and a silver wires (0.5 mm of diameter each one) were used as counter (CE) and quasi-reference electrodes (RE), respectively. A phosphate buffer solution (pH 6.9) was selected as electrolyte solution. The geometrical area of WE was fixed at 0.88 cm^2. Regarding to the LSV measurements, both CE and RE were directly immersed in a buffered droplet (20 µL) located onto the ITO electrode (WE). The electrical ITO contact was realized by a standard probe micromanipulator (Karl SÜSS probe station). All the electrical measurements on planar electrodes were performed by using an Agilent B1500A Semiconductor Device Analyzer at ambient conditions.

2.4 Patterning of the ITO electrodes

The whole photolithographic protocol was carried out in a 10000 class cleanroom. ITO-coated glass slides were firstly rinsed with acetone and isopropanol (HPLC pure grade), and afterwards dried with a nitrogen stream. The S1813 photoresist was spin-coated (spinning speed: 4000 rpm, spinning acceleration: 5700 rpm/s) and annealed on a hot-plate at 100 °C for 60 s. The electrodes pattern were designed using CAD (computer aided design) and transferred to the photoresist film by means of a laser-assisted writer (Durham magneto-optics, λ=405 nm). The substrates were then immersed in a solution of MF319 developer for 60 s and then washed with ultrapure water in order to remove the resist in the areas that had been exposed to the laser. An acidic etching (namely HCl 32% $^{v}/_{v}$ for 10 min) of the uncoated ITO was performed in order to define the designed electrodes. The resist was finally removed by rinsing with acetone and isopropanol.

2.5 Fabrication of μ-fluidics

The microfluidic device was fabricated by sticking a double-sided adhesive (90 μm thick) onto the modified glass-coated ITO electrodes. Its thickness defines the nominal volume of the micro-channels. A thermoformed polypropylene (90 μm thick) was used to ensure a proper reservoir for the aqueous droplet. In this way, the whole microfluidic system is completely closed. The double-sided adhesive tape was patterned by IR laser writer (Scriba) according to the different channel geometries. The micro-channels feature the following sizes: width 400 μm and length 4800/6800 μm. The microfluidic device used in cell manipulation has two 60 μL capacious reservoirs and channel dimensions of 600 μm width and 1000 μm length (Figure S1).

2.6 Cell culture

The NIH-3T3/GFP mouse embryonic fibroblast cell line (purchased from Cell Biolabs) was cultured in Dulbecco's modified eagle medium (DMEM), supplemented with 10% (v/v) fetal bovine serum, 2 mM L-glutamine, 100 IU/mL penicillin and 100 mg/mL streptomycin. The cell line was maintained in standard culture conditions (37°C in a humidified atmosphere with 5% CO_2). The cells were periodically sub-cultured using Trypsin-EDTA solution 0.25% for detachment process. Cells were seeded at density 9200 cells/mL, 20800 cells/mL, 41700 cells/mL, on the functionalized electrodes endowed3ee with microfluidics. Samples were examined using a Nikon Eclipse Ti-U microscope equipped for florescence analysis.

3. Results and discussion

The AQSi was chosen as active compound for this study and was synthesized according to the Scheme 1.[43] This molecule bears a triethoxysilane unit, as anchoring group towards oxide substrates, and an anthraquinone (AQ) moiety as electroactive core. AQ can be electrochemically reduced to the anthrahydroquinone (AQH_2) through a two-proton two-electron redox reaction in aqueous media[44] as follows:

$$AQ + 2H^+ + 2e^- \rightleftharpoons \mathrm{AQH_2}$$

AQSi-based SAMs (see experimental section and Figure 1a) were characterized by means of cyclic voltammetry (CV) (Figure 1b) in a phosphate buffer solution that guarantees a fixed pH equal to 6.9. The cathodic and anodic peaks fall at -0.74 V and -0.53 V (vs Ag(s)), respectively.

The electrochemical switch from *AQ* to *AQH_2* leads to the replacement of two carbonyl groups with two hydroxyl ones. The impact of this reaction on the surface wettability was checked by measuring the surface water contact angles (5 µL droplet), which were 60° for the *AQ* form and 34° for the AQH_2 (see Figure 1c-d). As expected, the latter form is more hydrophilic than the former one. This marked surface energy difference allowed us to study

the change of contact angle "*in-real time*". As a result, a three-contact electrochemical cell was set directly into the aqueous droplet (see experimental section). A linear potential ramp was applied spanning from 0 V to -0.9 V vs Ag(s). The electrowetting onset occurred at -0.6 V (Figure 2b and Video in Supporting Information) in agreement with the CV of the SAM (see Figure 1b). At this point, the spreading of the aqueous solution was clearly observed due to the formation of AQH_2. As benchmark test, a bare ITO electrode was also characterized by applying the same potential ramp, and no observable spreading of the water drop occurred. This cross-check enabled us to confirm that the difference in surface energy came from the redox reaction and we could rule out any possible influence of the ITO polarization in this potential window.

These first experiments do not move the droplet in a specific direction, because a sole SAM-coated electrode was conceived. In order to drive preferentially a water droplet towards a specific direction, two planar ITO electrodes were fabricated by photolithography and acid etching of the ITO. In particular, two SAM-coated ITO macro-electrodes with area equal to 12.5 mm^2 (Figure 3a) were realized. This new layout is well-suited for a directional actuation, but it loses partially the voltage control in the aqueous droplet due to the absence of a reference electrode. This first trial provides clearly all the evidences of an efficient actuation by means of the electrochemical switching properties of the SAM. By applying a bias ranging from 2.0 V to 2.2 V, an effective water actuation occurs. This new operational voltage stems from the lack of the reference electrode, as previously mentioned. Importantly, this voltage is still lower compared to the typical voltages used in EWOD systems[41] and hence AQ electroactive SAMs are attractive aiming at the fabrication of low-power and disposable technology. The preferential motion of the aqueous droplets is achieved towards the negative pole, as expected because of the AQ reduction giving rise to the more hydrophilic AQH_2. As reference test, the same planar configuration was tested by using the non-electroactive UTCS SAM instead of the AQSi. This inert SAM provides a perfect surface passivation and,

consequently, no droplet movement was observed in the same potential range. Thus, this experiment unambiguously proved that the dominant driving force acting for the water droplets actuation in the AQSi SAMs in the potential window used is the change of the molecular redox state that modulates the surface energy. However, it cannot be completely ruled out a small contribution of other effects such as capacitive processes.

With the goal of achieving more complex actuations such as droplets merging[45] an array of three coplanar ITO electrodes (*viz.* E1, E2 and E3) were designed (Figure 4a). Once the electrodes were functionalized with AQSi, two buffer droplets were placed acting as electrolytic bridges to close properly the electric circuit.

In order to get a more efficient visualization of the electrochemical actuation, two well-known dyes (*i.e.*, Fluorescein and Rhodamine 6G) were added in the solutions. E2 was grounded and a voltage equal to 2.8 V was applied to E1 and E3. According to the above-mentioned rationale, E2 is the negative pole wherein AQH_2 is formed yielding a gradient of surface tension responsible for the droplets merging (Figure.4b). It must be emphasized that 2.2 V is always the onset of the droplets movement; however, it has been observed that a slight higher bias (*i.e.*, 2.8 V) favors a faster water actuation. This experiment proves that the use of AQ-based SAMs can be exploited to promote droplets merging, which is one of the basic actuations demanded for digital µ-fluidics.

Aiming at bio-applications, it is required an overall miniaturization of the system due to the need of using small volumes of biological samples. Two usual problems have to be taken into account for handling smaller volumes: the first one is the proper control of the droplets volume and the second one is focused on avoiding adventitious contamination. These technical issues are connected to the dynamic equilibrium at the water/air interface, which might lead to water evaporation as well as an uncontrolled intake of contaminants. For this reason, we designed and fabricated a full-standing and compact chip, which is encapsulated into a microfluidic system capable to manage few micro-liters of solution (see Figure 5a for

the electrode layout and 5c,d for the chips employed). The SAM-guided motion was verified again in this self-standing chip, where an increased friction into the micro-channel takes place. The droplet was placed in the central reservoir of the microfluidics (E1) and by applying a voltage between the central electrode and one of the outer ones (*i.e.*, between E1 and E3 in Fig. 5b,d), hence the liquid movement towards the outer electrode was achieved. Importantly, the electrochemical actuation could be accomplished by using the same range of potential and without any detectable differences in motion speed. The system was further challenged on a more demanding task by using a fluidic channel featuring two sharp turns, with change of direction of the flow streamlines (Figure 5c). This new design forces the water flow along a contourted path, which could hamper it since the liquid could deviate along these additional paths because it is subjected to laminar flow. By applying a voltage between the electrodes E1 and E2 (see electrode layout in Figure 5e), the water droplet was successfully guided towards the desired direction. This proves that this chip offers a higher control on the water motion with respect to a standard microfluidic system connected to a peristaltic pump.

The successful implementation of a microfluidics onto the SAM-coated electrodes prompted us to explore its application for a relevant actuation in biology. For this reason, we aimed at moving a medium containing NIH-3T3 cells instead of a simple electrolytic solution. Firstly, we tested cell adhesion on chip for *in vitro* study in order to rate the adsorpion. We seed NIH-3T3 cells in complete medium (pH 7.4) with range of concentrations (from 2500 to 10000 cells/cm^2) and with incubation times of 5 min, 15 min, 6 h and 24 h. Once the cell adhesion was ensured, liquid motion of the droplet containing cells was followed by optical and fluorescence microscopy (see Figure 6). After 24 h, we observed that the cells remain attached to the device while retaining the morphology of fibroblasts. (see Figure 6b). No differences were observed in velocity compared to the liquid without the presence of cells. It has to be noted that the low range of potential required for the droplet actuation makes the system more compatible to cell culturing protocols. Furthermore, the voltage field

experimented by the cells during the actuation is always less than the applied voltage, indeed electrolysis of water is never observed. Although viability and adhesion are rough proofs of the effective state of the cell health, these preliminary results hint an efficient actuation, which will be matter of further investigations about more subtler details such as DNA damages, stress responses etc. Within this view, the effective gradient of cells from the starting well up to the micro-channel can be safely assumed as a proof-of-principle of our chip efficiency. The use of electrochemically active SAM turns out to be a promising approach for a controlled cell migration, which is fundamental to many physiological processes, such as regeneration, tissue repair and protective immunity.[46]

4. Conclusions

In summary, the electrowetting properties of AQSi based SAMs on ITO were successfully implemented into a micro-electromechanical system (MEMS). The two-proton two-electron redox reaction associated to the AQ core is the driving force for water actuation. The switchable electrodes have been successfully miniaturized and endowed with a microfluidic system on top. The here-reported smart electrodes reveal important figure of merits, such as transparency, robustness and bio-friendliness. Furthermore, the driving voltages are matching the best digital microfluidics based on standard dielectrics (*i.e.* few volts), but some sophistications can be implemented in order to optimize the ratio efficiency/power consumption. It should be highlighted that by chemical synthesis it should be possible to prepare molecules showing two accessible redox states with more distinct hydrophilic/hydrophobic properties and, hence, the residue remaining during droplet manipulation would be minimized and the reversibility of the system improved. Thus, the functionalization of ITO-based chips with electroactive molecules constitute a promising platform to be implemented in digital microfluidics as an alternative option to conventional pumping systems or even EWOD-based device composed by standard plastic dielectrics.

Furthermore, the efficient actuation of NIH-3T3 medium makes our technology extremely promising towards bio-applications.

References

[1] S. Casalini, C.A. Bortolotti, F. Leonardi and F. Biscarini, *Chem. Soc. Rev*.**2017**, *46*, 40-71.

[2] C. E. D. Chidsey, C. R. Bertozzi, T. M. Putvinski and A. M. Mujsce, *J. Am. Chem. Soc.* **1990**, *112*, 4301-4306.

[3] A. L. Eckermann, D. J. Feld, J. A. Shaw and T. J. Meade, *Coord. Chem. Rev.* **2010**, *254*, 1769-1802.

[4] Z. Liu, A. A. Yasseri, J. S. Lindsey and D. F. Bocian, *Science* **2003**, *302*, 1543-1545

[5] Y. B. Zheng, B. K. Pathem, J. N. Hohman, J. C. Thomas, M. Kim and P. S. Weiss, *Adv. Mater.* **2013**, *25*, 302-312.

[6] M. Mas-Torrent, C. Rovira and J. Veciana, *Adv. Mater*.**2013**, *25*, 462-468.

[7] E. Marchante, N. Crivillers, M. Buhl, J. Veciana and M. Mas-Torrent, *Angew. Chem. Int. Ed.* **2016**, *55*, 368-372.

[8] C. T. Cioffi, A. Palkar, F. Melin, A. Kumbhar, L. Echegoyen, M. Melle-Franco, F. Zerbetto, G. M. A. Rahman, C. Ehli, V. Sgobba, D. M. Guldi and M. Prato, *Chem. A. Eur. J.* **2009**, *15*, 4419-4427.

[9] M. Fibbioli, K. Bandyopadhyay, S-G. Liu, L. Echegoyen, O. Enger, F. Diederich, P. Buhlmann and E. Pretsch, *Chem. Commun.* **2000**, *5*, 339-340.

[10] C. Simão, M. Mas-Torrent, J. Casado-Montenegro, F. Otón, J. Veciana and C. Rovira, *J. Am. Chem. Soc.* **2011**, *133*, 13256-13259.

[11] K. M. Roth, J. S. Lindsey, D. F. Bocian and W. G. Kuhr, *Langmiur* **2002**, *18*, 4030-4040.

[12] W-S Yeo and M. Mrksich, *Langmuir* **2006**, *22*, 10816-10820.

[13] M.N. Yousaf and M. mrksich, *J. Am. Chem. Soc.***1999**, *121*, 4286–4287.

[14] J. Casado-Montenegro, E. Marchante, N. Crivillers, C. Rovira and M. Mas-Torrent, *ChemPhysChem* **2016**, *17*, 1810-1814.

[15] S. A. Trammell, D. S. Seferos, M. Moore, D. A. Lowy, G. C. Bazan, J. G. Kushmerick and N. Lebedev, *Langmuir* **2007**, *23*, 942-948

[16] J.A.M. Sondag-Huethorst and L.G.J. Fokkink, *Langmuir* **1992**, *8*, 2560-2566.

[17] J. A. M. Sondag-Huethorst and L. G. J. Fokkink, *J. Electroanal. Chem.* **1994**, *367*, 49-57.

[18] N. L. Abbott and G. M. Whitesides, *Langmuir* **1994**, *10*, 1493-1497.

[19] J. A. M. Sondag-Huethorst and L. G. J. Fokkink, *Langmuir* **1994**, *10*, 4380-438719.

[20] C. Simão, M. Mas-Torrent, J. Veciana and C. Rovira, *Nano Lett.* **2011**, *11*, 4382-4385

[21] J. Casado-Montenegro, M. Mas-Torrent, F. Otón, N. Crivillers, J. Veciana and C. Rovira, *Chem. Commun.* **2013**, *49*, 8084-8086.

[22] W. H. Mulder, J. Calvente and R. Andreu, *Langmuir* **2004**, *20*, 869-874.

[23] C. B. Gorman, H. A. Biebuyck, G. M. Whitesides, *Langmuir* **1995**, *11*, 2242-2246.

[24] V. Pretorius, B.J. Hopkins, J.D. Schieke *J. Chromatog.* **1974**, *99*, 23-30

[25] Y. Ren,W. Liu,Y. Jia,Y. Tao, J. Shao,Y. Ding and H. Jiang, *Lab Chip* **2015**, *15*, 2181-2191

[26] G. Beni, M. Tenan *J. Appl. Phys.* **1981**, *52*, 6011-6015

[27] H Richter, H. Sandmaier *IIEE Int. Conf. Micro Electro Mech. Syst.* **1990**, IEEE, 99-104

[28] W. Liu, Y. Ren, J. Shao, H. Jiang, Y. Ding *J. Phys. D: Appl. Phys.* **2014**, *47*, 075501

[29] Y. Ren, H. Jiang, H. Yang, A. Ramos, P. García-Sanchez, *J. Electrost.* **2009**, *67*, 372–376.

[30] A. Salari, M. Navi, C. Dalton, *Biomicrofluidics* **2015**, *9*, 1-14.

[31] A Ramos, H Morgan, N G Green and A Castellanos, J. Phys. D: Appl. Phys. **1998**, *31*, 2338–2353.

[32] J. Lee, H. Moon, J. Fowler, T. Schollhammer and C. J. Kim, *Sens. Actuators A* **2002**, *95*, 259-268.

[33] M. G. Pollack, R. B. Fairalexander, D. Shenderov, R. B. Fair and A. D. Shenderov, *Appl. Phys. Lett*. **2000**, *77*, 1725-1726.

[34] V. Srinivasan, V. K. Pamula and R. B. Fair, *Anal. Chim. Acta* **2004**, *507*, 145-150.

[35] D. Mark, S. Haeberle, G. Roth, F. Von Settenz and R. Zengerle, *Chem. Soc. Rev.* **2010**, *39*, 1153-1182.

[36] G. J. Shah, A. T. Otha, E. P. Y. Chiou, M. C. Wu and CJ Kim, *Lab Chip* **2009**, *9*, 1732-1739.

[37] I. Barbulovic-Nad, H. Yang, P. S. Park and A. R.Wheeler, *Lab Chip* **2008**, *8*, 519-526.

[38] W. C. Nelson and CJ Kim, j. Adhes. *Sci. Technol.* **2012**, *26*, 12-17.

[39] M. Abdelgawad, A. R. Wheeler, *Adv. Mater.* **2009**, *21*, 920–925.

[40] Y.You Lin, E. R. F. Welch, R. B. Fair, *Sensors and Actuators B **2012**, 173, 338– 345.*

[41] H. Moon, S. Kwon Cho and R. L. Garrell, *J. Appl. Phys.* **2002**, *92*, 4080-4087.

[42] S. Casalini, M. Berto, C. A. Bortolotti, G. Foschi, A. OPeramolla, M. Di Lauro, O. H. Omar, A. Liscio, L. Pasquali, M. Montecchi, G. M. Farinola and M. Bosari, *ACS Appl. Mater. Interfaces* **2015**, *7*, 3902-3909.

[43] P. Saint-Cricq, T. Pigot, L. Nicole, C. Sanchez and S. Lacombe, *Chem. Commun.* **2009**, *35*, 5281-5283.

[44] S. I. Bailey and I. M. Ritchie, *Electrochim. Acta* **1985**, *30*, 3-12.

[45] R. G. Pollak, A. D. Shenderov and R.B Fair, *Lab Chip* **2002**, *2*, 96-101.

[46] D. Webb and R. Horwitz, *Curr. Biol.* **2003**, *13*, R756-R759

Acknowledgements

This work was funded by the ITN iSwitch 642196, ERC StG 2012-306826 e-GAMES, Networking Research Center on Bioengineering, Biomaterials, and Nanomedicine (CIBER-BBN), the DGI (Spain) project FANCY CTQ2016-80030-R, the Generalitat de Catalunya (2014-SGR-17) and the Spanish Ministry of Economy and Competitiveness, through the "Severo Ochoa" Programme for Centers of Excellence in R&D (SEV-2015-0496). M. S. M. is enrolled in the Materials Science PhD Program of Universitat Autònoma de Barcelona. S.C. acknowledges the People Programme (Marie Curie Actions) of the Seventh Framework Programme of the European Union (FP7/2007-2013) under Research Executive Agency Grant Agreement No. 600388 (TECNIOSpring programme), and from the Agency for Business Competitiveness of the Government of Catalonia, ACCIÓ.

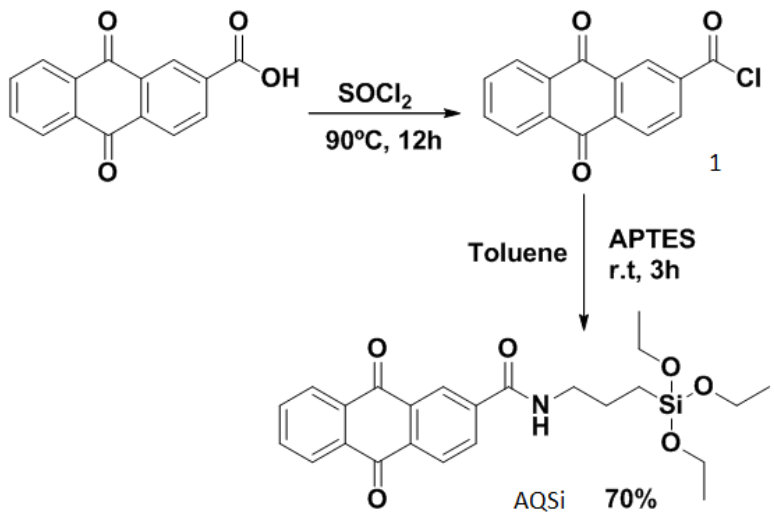

Scheme1 Synthetic pathway to prepare AQSi.

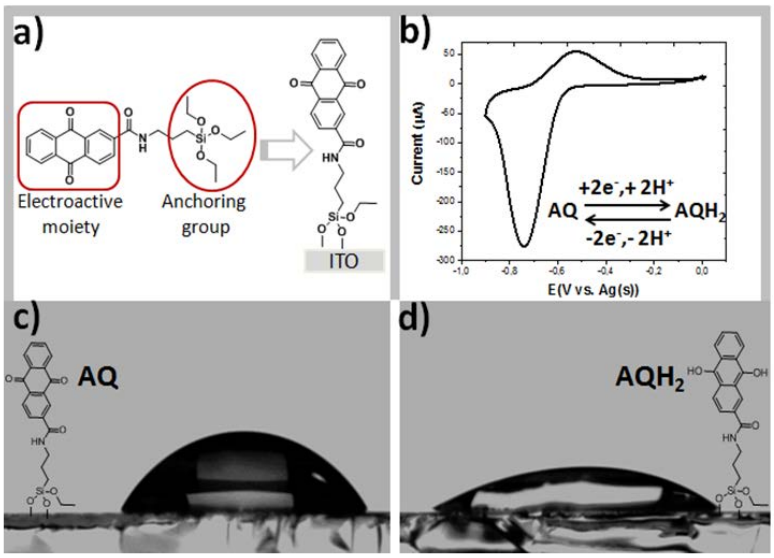

Figure 1 a) Molecular structure of AQSi and scheme of the AQSi-SAM on ITO. b) Cyclic voltammogram of AQSi SAM-coated ITO electrode in a phosphate buffer solution at pH~6.9. c) Optical images of the water droplets (5 µL) before and d) after the electrochemical reduction of the SAM.

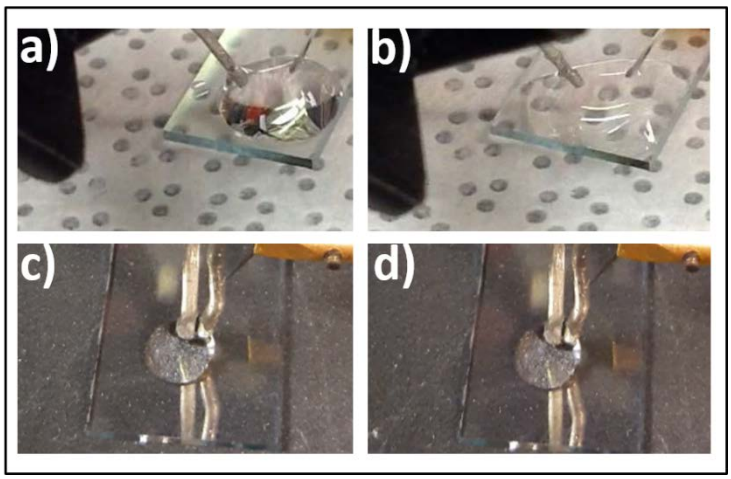

Figure 2 Initial (a,c) and final (b,d) state of the electrowetting onto AQSi-coated ITO (a,b) and on bare ITO (c,d).

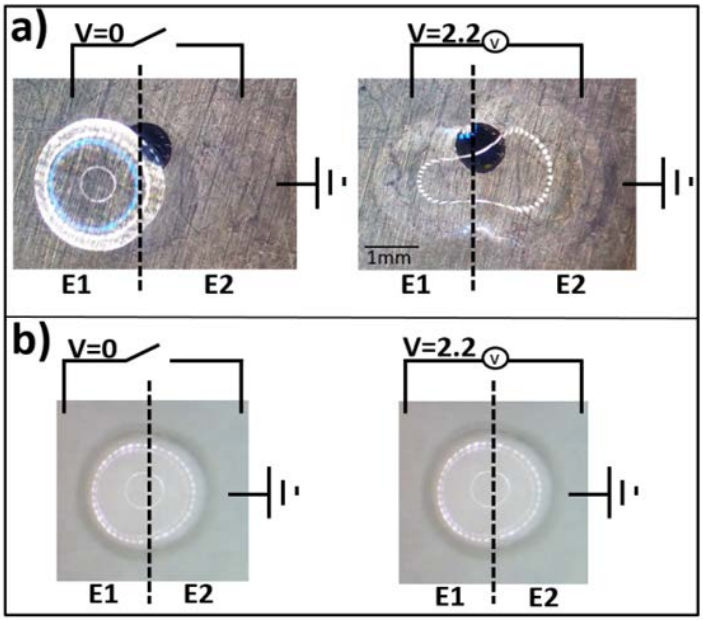

Figure 3 Optical images of AQSi-coated (a) coplanar ITO electrodes and (b) UTCS-coated ones. On the left, both images show the open circuit state. On the right, both images show the biased state, namely a voltage difference equal to 2.2 V. The black dotted line stands for the separation of the electrodes.

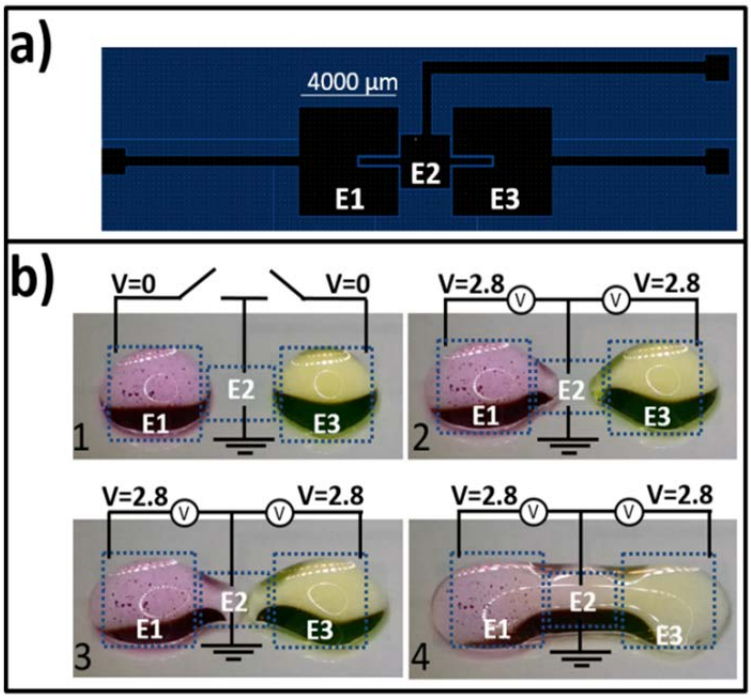

Figure 4 a) CAD drawing of the three-electrode array. b) Snapshots of the droplet merging.

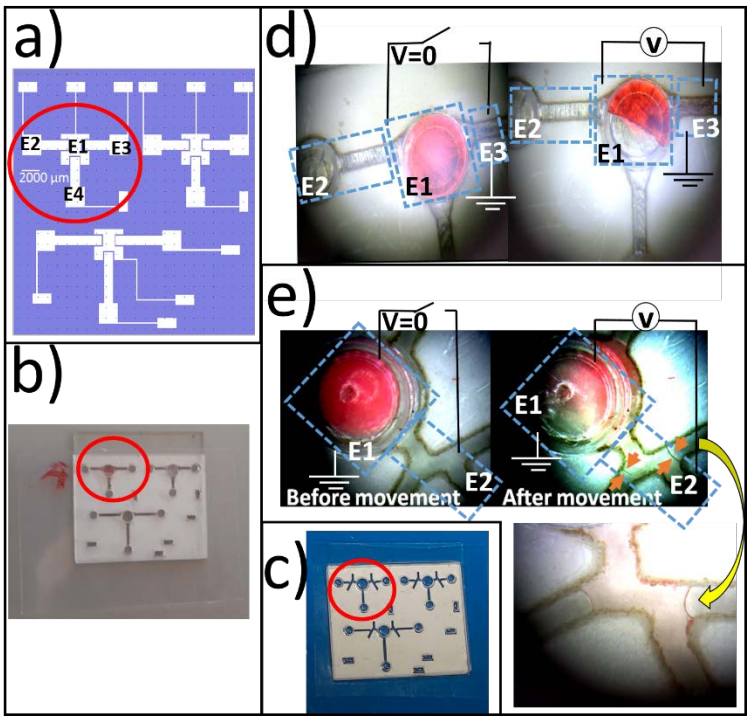

Figure 5 a) CAD drawing of the three-electrode array. b), c) Optical image of the employed self-standing chips. d) Optical image of the SAM-guided droplet motion. e) Optical image of the contorted flow. The orange arrows define the edge of the water droplet that coincides with the border of the electrode.

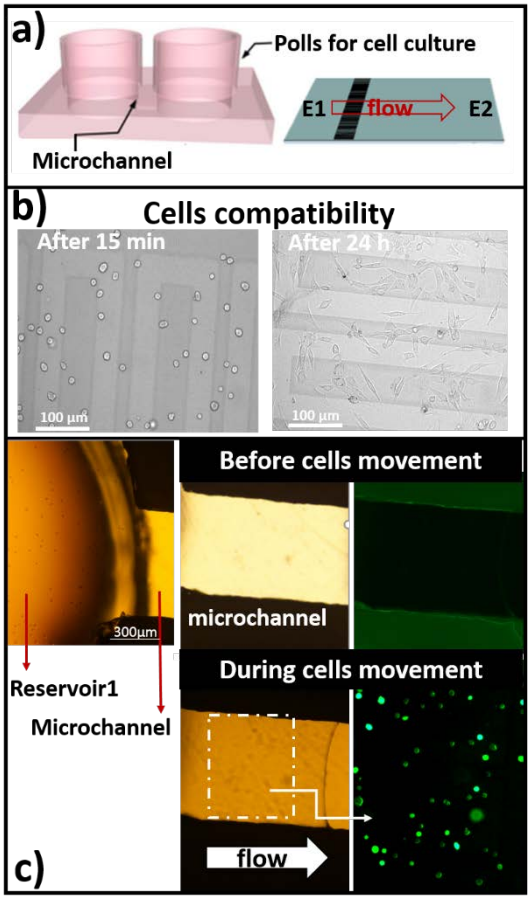

Figure 6 a) Microfluidic device used for cells manipulation including a simple microfluidic channel between two cells reservoirs placed in direct contact with ITO functionalized with AQSi-SAM. b) Cells in the microfluidic device after 15 min and 24 h. c) Movement of cells in the culture medium from one to the other reservoir upon the application of the electrowetting potential.

TOC